

Dipolar Driven NMR

S. Clough and K.J. Abed

*Department of Physics
University of Nottingham
Nottingham, NG7 2RD, England*

Contents

I. Introduction	3
II. Measurement of Tunnel Frequencies	4
III. Measurement of T_1 at Low Field	4
IV. Higher Order Transitions	7
V. Polarization Transfer from Rotational Polarization	7
VI. Rotational Pressure	8
VII. Rotational Friction	9
VIII. Vector Potential	9
IX. References	10

I. Introduction

At high fields the axis of the spin quantization of a nuclear spin system is determined by the direction of the external field. As a result, the dipolar interactions are sharply divided into secular and non-secular parts. At low fields (or in the rotating frame), an oscillating field perpendicular to the main field may easily tilt the quantization axis, with the consequence that part of the dipole-dipole interactions become time dependent with a frequency equal to that of the oscillating field, or harmonics of that frequency. These time dependent terms may then drive transitions, with selection rules characteristic of the dipole-dipole matrix elements (1). This contrasts with the high field case where transitions are driven directly by the r.f. field. Because the dipole-dipole Hamiltonian is much richer in matrix elements, the low field spectra are more complicated and provide new opportunities to study molecular motion at low temperatures.

Dipolar driven transitions are of course familiar from the theory of spin lattice relaxation, but in this case the driving energy comes from a broad noise spectrum associated with motion, and only a single parameter T_1 is measured. In contrast the low field spectroscopy is coherent so the different parts of the dipole-dipole interactions give rise to well resolved transitions.

A disadvantage of low field NMR is that it is necessary to use rapid field cycling techniques so that the initial preparation of a magnetic state, and the subsequent measurement of the result of perturbing it at low field, can both be carried out at high field. This means that the spin lattice relaxation time T_1 must not be short compared with the total experiment time which includes the field switching. Since many of the most interesting fundamental problems must anyway be studied at low temperatures when T_1 may be many minutes, this is not too severe a restriction. A typical experimental sequence consists of (1) a high field preparation period T_p initiated

by a magnetization destroying comb of resonant r.f. pulses to establish a well defined starting condition, (2) a low field period t_d during which a r.f. field at frequency ω is switched on and the magnetism may be partly destroyed, (3) a measurement of M_z at high field using a single 90° inspection pulse. The field switching is accomplished in a few seconds (typically 2–5 s) in most of our data. Most of our experiments have been carried out at 4.2 K and the long relaxation times necessitate a long value of t_p to enable an adequate magnetization to grow. A magnetization destruction spectrum is obtained by repeating the cycle many times and incrementing or decrementing the low field value B . All other elements of the sequence are unchanged. Different scans may be obtained with different values of ω , so that finally a two-dimensional spectrum $f(B, \omega)$ is obtained. The spectra consist of negative peaks on a flat or fairly smooth background. The most prominent are the $\Delta m = 1$ and $\Delta m = 2$ peaks at $B = \omega/\gamma$ and $B = \omega/2\gamma$. Sidebands due to tunnelling methyl groups occur at $B = (\omega \pm \omega_t)/\gamma$ and $(\omega \pm \omega_t)/2\gamma$ and are referred to as $\Delta m = 1$ and $\Delta m = 2$ sidebands. They offer a very simple and precise way of measuring the tunnel splittings ω_t and a large number of such measurements have now been made. The accuracy of such measurements is normally about ± 5 kHz.

In addition to the effects of the r.f. field, the magnetization evolves at low field due to other factors. One of these is spin lattice relaxation which may be much more rapid at low field than at high field. Since the equilibrium magnetization is also known to be nearly zero, it is a simple matter to measure T_1 at low field and low temperature. This is again in contrast to the case at high field where very long times are needed to establish the equilibrium magnetization and measurements of T_1 are difficult. Another low field effect occurs with rotating molecular groups where a magnetization change during the preparation period may induce a population difference between spin symmetry species. The lowered entropy can be shared with the nuclear Zeeman system at a field which makes Zeeman and dipolar splittings similar, resulting in an enhanced nuclear magnetization. Since both the r.f. field and nuclear spin lattice relaxation normally destroy magnetization, the observed growth of the magnetization is a clear signature of an effect of this kind.

II. Measurement of Tunnel Frequencies

Figures 1 and 2 show typical spectra for a number of ketones and alkanes. The $\Delta m = 1$ and $\Delta m = 2$ peaks are labelled A and B and their tunnel sidebands by a and b. The derived tunnel frequencies are given in the figure captions. In some cases it is not clear whether multiple tunnel peaks result from different kinds of methyl groups in the unit cell, or from a structure due to mechanical coupling between two or more groups. This is an active area of present study.

Three general conclusions follow from these and similar results. The first is that CH_3 groups attached to sp^3 atoms are always strongly hindered with tunnel frequencies of a few hundred kHz or less, while those attached to sp^2 atoms are much less hindered. The second is that the sp^3 tunnel frequencies fall in a relatively narrow window of the (logarithmic) tunnel frequency range. This again points to the origin of the hindering barrier being internal to the molecule. The wide spread of sp^2 tunnel frequencies indicates a weak intramolecular contribution with the barrier mainly due to structure dependent intermolecular interactions. The third conclusion is that all the collected data strongly reinforces the previously observed correlation between frequency and hopping rate (2) as measured by the temperature dependence of T_1 . All the samples in Figures 1 and 2 exhibit T_1 minima in the range 120 K – 160 K with the temperature correlated with the tunnel frequency. This demonstrates again that the hopping rate at a particular temperature is just a measure of the transparency of the potential barrier at a height above the minimum related to the temperature (3).

III. Measurement of T_1 at Low Field

Figure 1 shows spectra of 2-hexanone and 2-heptanone. The fall in the magnetization at low field is due to spin lattice relaxation which occurs in these samples due to the random reorientation of the weakly hindered sp^2 methyl group whose tunnel frequencies have been measured by neutron scattering. By varying the duration of the period spent at

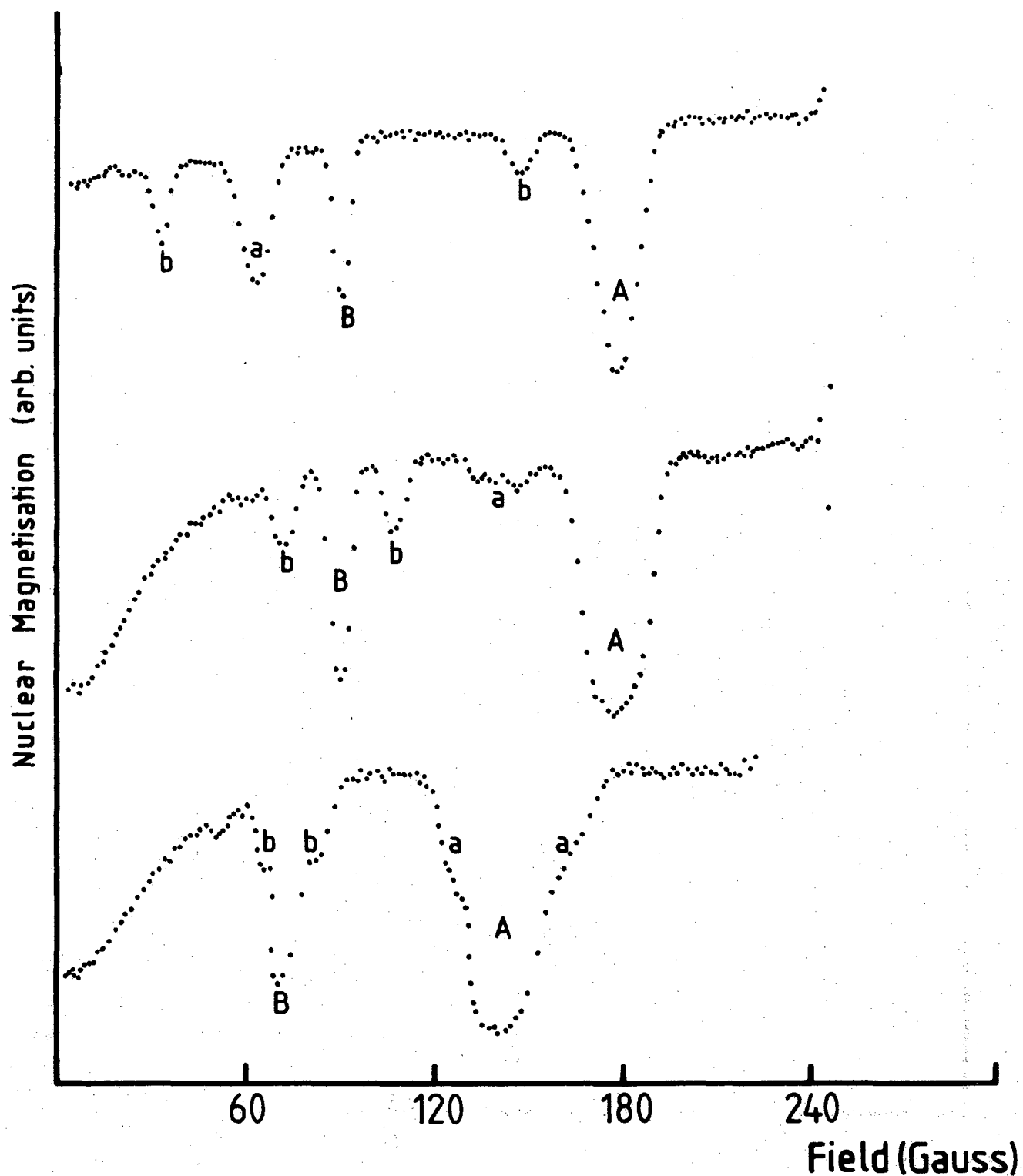


Figure 1. Dipolar driven NMR spectra from 2-butanone (top), 2-hexanone and 2-heptanone (bottom). For the first two a frequency of 750 kHz was used and 600 kHz for the last. Each shows one pair of methyl tunnel sidebands on the $\Delta m = 1$ (A) and $\Delta m = 2$ (B) peaks. The tunnel frequencies are 495 kHz, 152 kHz and 63 kHz.

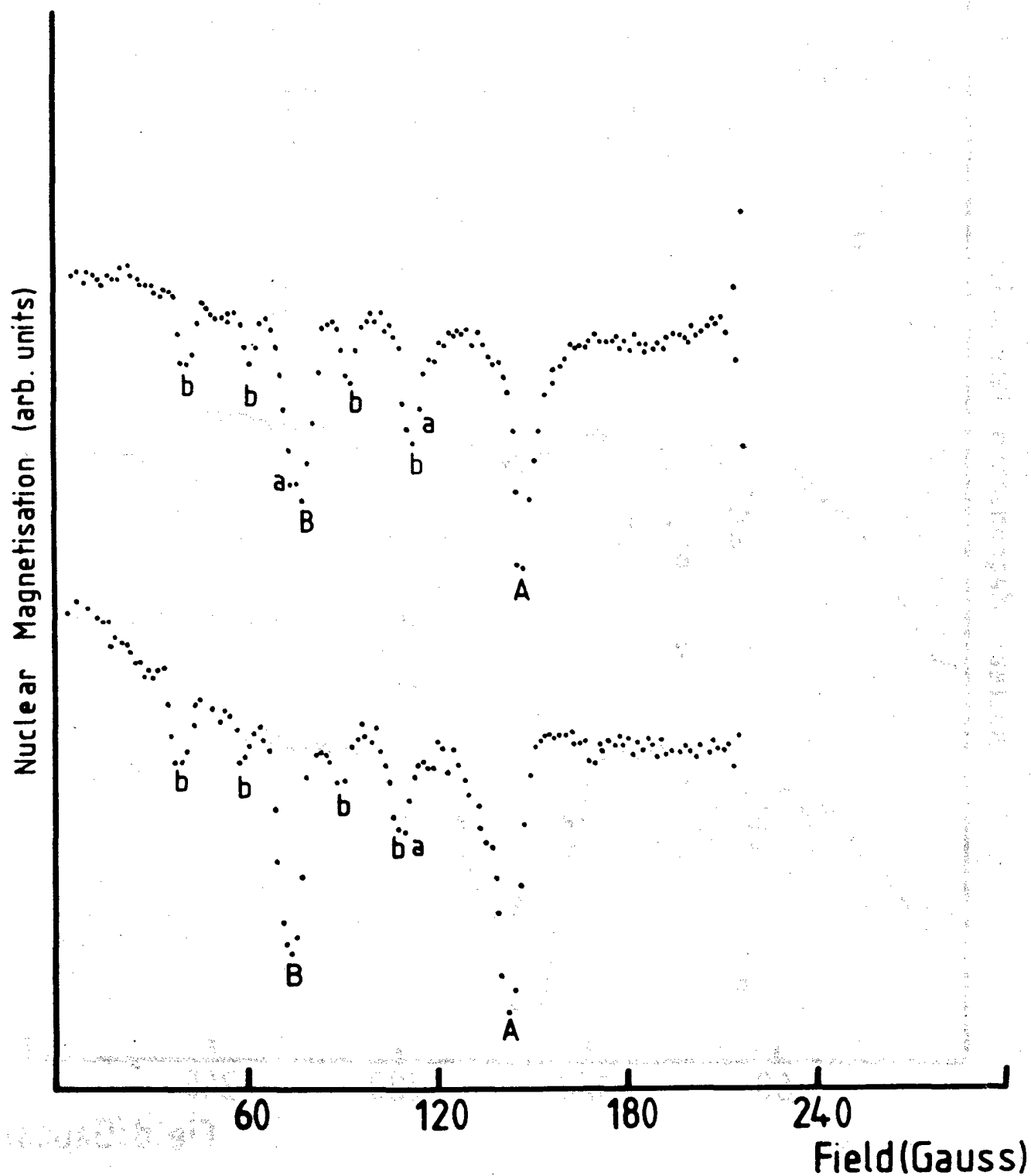


Figure 2. Dipolar driven nmr spectra for heptane (top) and nonane (bottom). A frequency of 600 kHz was used which determines the position of the $m = 1$ and 2 transitions A and B. Each shows two sets of tunnel sidebands with tunnel frequencies 146 and 298 kHz for heptane, and 134 and 299 kHz for nonane.

low field, T_1 and its field dependence can be found.

IV. Higher Order Transitions

Although the main peaks can be attributed to $\Delta m = 2$, the transition at $\Delta m = 3$ can often be detected and care needs to be taken to avoid attributing it to a sideband. Its dependence on ω clearly identifies it.

Since there are no $\Delta m = 3$ matrix elements in the dipole-dipole interaction, it is explicable only in second order perturbation theory. Its appearance illustrates the sensitivity of the technique. Associated with the $\Delta m = 3$ can be weak sidebands at $B = (\omega \pm \omega_t)/3\gamma$ and even $B = (\omega \pm 2\omega_t)/3\gamma$ which implies a transition converting two methyl groups.

V. Polarization Transfer from Rotational Polarization

Figure 2 shows in contrast to Figure 1 a case (nonane) where the magnetization grows at low field. This requires that T_1 be long since the equilibrium magnetization is near zero. This observed change is an isentropic one. It demonstrates that the system after preparation at high field has some kind of order other than that associated with M_z . For tunnelling methyl groups, this can be identified as associated with the difference in population of the E^a and E^b spin symmetry species. This is rotational polarization (4). It implies a non-zero mean value of angular velocity since the E^a and E^b states have opposite angular momenta.

Terms in the dipolar Hamiltonian exist which can interconvert E^a and E^b species and also flip nuclear spins, but at low temperature there is no energy source to drive the change in Zeeman energy occurring in these transitions. The rotational polarization is therefore quasi-invariant except at very low fields. When the nuclear Zeeman splitting is comparable with the dipolar energies, then an exchange of entropy can occur because the dipolar reservoir provides the energy required for the transition. The reduced entropy manifests itself as enhanced magnetization when the field is again increased. By observing the effect as a function of time, the relaxation of the rotational polarization can be studied at different fields.

The nature of rotational polarization is illustrated in Figure 3 which shows the energy levels of a methyl group. Apart from the usual nuclear Zeeman splitting, there is a tunnel splitting of the A species (total nuclear spin 3/2) from the two E species, E^a and E^b , each of which has a total nuclear spin 1/2. The tunnel splitting arises from the different rotational energies of the states, the rotation being by quantum mechanical tunnelling through the hindering barrier. It is this splitting which is responsible for the tunnelling satellites in Figures 1 and 2. The intra-methyl group dipole-dipole interactions have a helical character, illustrated in Figure 3 by the transition probabilities T and T'. Since these are generally different, it follows that a change in magnetization is accompanied by a change in the population difference of the two E species.

The E^a and E^b wavefunctions have equal and opposite angular momenta, so an unequal weight means that the methyl groups have acquired a rotational motion with a particular sense. What has occurred is that some of the angular momentum associated with the nuclear magnetization has been transferred during relaxation to rotation of the methyl group itself. This rotational polarization is generated during the preparation period of the experiment at high field. If the field is reduced to a sufficiently low value, then the non-secular dipole-dipole terms are able to scramble the populations in a way which conserves the total entropy. When the high field is restored all of the order goes into the Zeeman reservoir.

The energies and populations of the eight levels can be simply described by using two sets of quantum numbers. In addition to the magnetic quantum number m , we define $\mu = 1, 0, -1$ for E^a, A, E^b states. Then m takes the values 3/2, 1/2, -1/2, -3/2 for $\mu = 0$ and is otherwise restricted to 1/2, -1/2. The energies of the 8 levels are

$$E(m, \mu) = -\hbar\omega_0 m - \hbar\omega_t \left(\frac{1}{2} - \mu^2\right) \quad (1)$$

where ω_0 is the Larmor frequency and ω_t the tunnel frequency. The fractional populations can be written (in the high temperature approximation) in terms of three parameters

$$n = \frac{1}{8} (1 + \beta_z m + \beta_t (\frac{1}{2} - \mu^2) + R\mu) \quad (2)$$

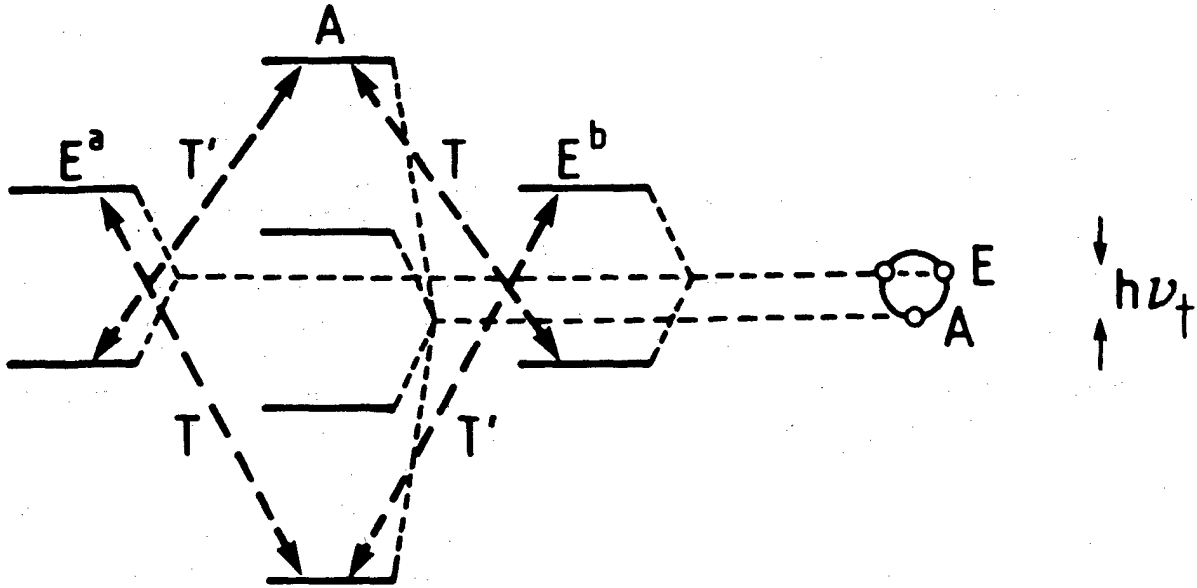


Figure 3. The energy levels of a methyl group at low temperature. The two E species lie above the A species by the tunnel splitting. The symmetry of dipolar matrix elements is indicated by the symbols T and T' which are generally different. The result is that a change in nuclear magnetization can induce a difference in the population of the two E species. This is rotational polarization.

The parameters β_z and β_t define Zeeman and tunnelling temperatures through

$$\begin{aligned}\beta_z &= \hbar\omega_o/kT_z \\ \beta_t &= \hbar\omega_t/kT_t\end{aligned}\quad (3)$$

We shall discuss the meaning of R in the next section.

The entropy S is given by

$$S/k = -\sum n \ln(n) \simeq \ln 8 - \frac{3}{4}\beta_z^2 - \frac{1}{4}\beta_t^2 - \frac{1}{2}R^2 \quad (4)$$

where the coefficients come from summing m^2 , $(\frac{1}{2} - \mu^2)^2$, μ^2 .

Following demagnetization and remagnetization, this is converted to

$$S/k = \ln 8 - \frac{3}{4}\beta_z'^2 \quad (5)$$

$$\beta_z' = [\beta_z^2 + \frac{1}{3}(\beta_t^2 + 2R^2)]^{\frac{1}{2}} \quad (6)$$

This is the enhancement in the nuclear magnetization.

VI. Rotational Pressure

A meaning for the parameter R can be found by comparing the thermodynamic relation $S = f(U, R)$ with that for a gas $S = f(U, V)$. Since in the latter case $-(\partial U/\partial V)_S$ is the pressure p, we can identify $-(\partial U/\partial R)_S = p_R$ as a negative internal rotational pressure, its sign being such that it tends to drive R to zero. The energy is given by

$$U = \sum nE(m, \mu) = -\frac{3}{4}\beta_z\hbar\omega_o - \frac{1}{4}\beta_t\hbar\omega_t \quad (7)$$

and in thermal equilibrium $\hbar\omega_o\beta_t$ so

$$p_R = \hbar\omega_o \left[\frac{3}{4} + \frac{1}{4}(\omega_t^2/\omega_o^2) \right] (\partial\beta_z/\partial R)_S \quad (8)$$

$$p_R = -kTR/2 \quad (9)$$

This represents the tendency of the rotational polarization to decline, thereby increasing the entropy of the system. The Gibbs free energy takes the form

$$G = U - TS + p_R R \quad (10)$$

VII. Rotational Friction

If a rotating molecule in a crystal acquires a rotation in a definite sense, in response to the changing magnetization, then it is reasonable to inquire if the rotation occurs with or without dissipation. The way the dissipation arises is through a phase shift of the wavefunction of the rotor which comes from the fact that the rotor is driving the environment. This is an example of Berry's topological phase (5) which occurs in all driven quantum mechanical systems. The phase shift depends on the geometry of the path. It breaks the usual boundary condition $\psi(\varphi) = \psi(\varphi + 2\pi)$ which applies only to isolated systems, and also breaks time reversal symmetry. The physical effect of this phase shift is that of a resistive torque and a consequence is to lift the degeneracy of the E levels. The broadening of the motional spectrum with increasing temperature is a manifestation of the fluctuating splitting of the E levels associated with a thermally fluctuating lattice-generated torque. At the same time the rotational states become localized and one passes smoothly with increasing temperature from coherent wave-like tunnelling states to localized states moving incoherently between potential wells in response to the fluctuating torque.

This provides a justification for the simple hopping model of molecular rotation usually employed at high temperatures, and illustrates that it is entirely consistent with the quantum mechanical model outlined here.

Before the enormous amount of recent work on Berry's phase, the situation has been confused and controversial because the boundary condition $\psi(\varphi) = \psi(\varphi + 2\pi)$ was frequently assumed to apply even in solids at high temperature when the angular momentum of the rotor is far from being a constant of the motion. Now it can be seen that the effect of this assumption is to eliminate driving effects, torques and dissipation.

The temperature dependence of the magnitude and frequency spectrum of the lattice induced torque is a topic of considerable interest. It is undoubtedly linked to the degree of vibrational excitation (4) though the details of this connection are still to be established. So far as the parameters of the last section is concerned one may assume:

$$p_R = -\left(\frac{1}{2}kT + \lambda\right)R \quad (11)$$

where λ is a coefficient of rotational friction.

VIII. Vector Potential

The most illuminating view of the topological phase factors arising because of the driving effects at the interface of rotor system and environmental heat bath is that they can be ascribed to a vector potential term in the Hamiltonian. Wilczek and Zee (6) have shown that a gauge theory structure is implicit in driven dynamics. This puts the elastic forces in solids on the same footing as all other forces in nature - all arise in the context of gauge theory. Methyl rotation is the simplest case and has an Abelian structure like electromagnetism. More complex molecular motions require the Yang-Mills non-Abelian gauge structure. In either case though, a new and thoroughly explored theoretical framework is now available to describe thermally driven molecular motions.

The vector potential depends on the velocities of the neighbouring atoms just as the scalar potential depends on their positions. The kinetic term becomes

$$\frac{1}{2I} \left(i\hbar \frac{\partial}{\partial \varphi} + I\omega \right)^2$$

where the vector potential $I\omega$ is proportional to the integral of the environmental torque. As the explicit appearance of i indicates, it has the effect of breaking the time reversal symmetry and thereby lifting the degeneracy of the two E levels. This discriminates between right handed and left handed rotation in response to the definite sense of rotation associated with a change of a particular sign in the nuclear magnetization. The splitting of the E levels leads to a broadening of the NMR line whose shape therefore depends on the integral of changes of magnetization immediately before measurements. In this way the nuclear magnetic resonance spectrum of a rotating molecule gives information, not only on its own motions, but also on the driving motions of the environment. This enables one to think of a rotating molecule as a kind of microscopic viscometer, to which a torque can be applied by changing the magnetization via the dipole-dipole interactions, causing

rotational motions of molecule and correlated motions in the environment through the viscous drag. Dipole-dipole driven NMR offers the best opportunity of observing effects of this kind and results supporting this general picture have been published elsewhere (7).

IX. References

¹S. Clough, A. J. Horsewill, P. J. McDonald and F. O. Zelaya, *Phys. Rev. Letters* **55**, 1794 (1985).

²S. Clough, A. Heidemann, A. J. Horsewill, J. D. Lewis and M. N. J. Paley, *J. Phys. C: Solid State Phys.* **4**, L525 (1981).

³S. Clough, A. Heidemann, A. J. Horsewill, J. D. Lewis and M. N. J. Paley, *J. Phys. C: Solid State Phys.* **15**, 2495 (1982).

⁴S. Clough, P. J. McDonald and F. O. Zelaya, *J. Phys. C: Solid State Phys.* **17**, 4413 (1984).

⁵M.V. Berry, *Proc. Roy. Soc. A* **392**, 45 (1984).

⁶F. Wilczek and A. Zee, *Phys. Rev. Lett.* **52**, 2111 (1984).

⁷S. Clough, G. J. Barker, K. J. Abed and A. J. Horsewill, *Phys. Rev. Lett.* **60**, 136 (1988).